JOURNAL OF AGRICULTURAL AND FOOD CHEMISTRY

Physical Aging of Starch, Maltodextrin, and Maltose

TIMOTHY R. NOEL,† ROGER PARKER,† GEOFFREY J. BROWNSEY,†
IMAD A. FARHAT,‡ WILLIAM MACNAUGHTAN,‡ AND STEPHEN G. RING*,†

Institute of Food Research, Norwich Research Park, Norwich NR4 7UA, United Kingdom, and Division of Food Sciences, University of Nottingham, Sutton Bonington Campus, Loughborough, Leicestershire LE12 5RD, United Kingdom

The physical aging of low water content, amorphous starch/water, maltodextrin/water, and maltose/water mixtures in the glassy state was examined using mechanical testing and calorimetry. Stress relaxation measurements showed that upon storage of the glassy materials there was a time-dependent increase in both flexural modulus and mechanical relaxation time. The mechanical relaxation time increased with depth of quench below the calorimetric glass transition temperature and with aging time at the quench temperature. Calorimetry of the aged materials showed an overshoot in heat capacity in the vicinity of the glass transition. The logarithm of the mechanical relaxation time showed a simple linear relationship with the size of the overshoot expressed as an enthalpy change. The calorimetric behavior could be modeled using the Tool−Narayanaswamy−Moynihan method.

KEYWORDS: Starch; maltodextrin; maltose; glass; physical aging

INTRODUCTION

Starch and its hydrolysates have widespread use as food ingredients. The physical stability of the resulting products has an important impact on shelf life. For starchy materials of intermediate water content, containing 20−95% w/w water, the phase separation and crystallization of starch chains at ambient temperatures lead to time-dependent changes in material properties. This process involves both amylose and amylopectin and is collectively known as retrogradation (*1*). Low moisture systems may also be subject to time-dependent change due to the phenomenon of physical aging or structural relaxation (*2*−*8*). The phenomenon occurs in a range of food materials and natural biopolymers systems (*2*, *5*, *8*). For synthetic materials, this phenomenon has been extensively studied (*9*, *10*).

Low moisture amorphous starchy materials and maltodextrins are often glassy at ambient temperatures (*11*, *12*). A glass has solidlike characteristics with a liquidlike structure. If a low molecular weight carbohydrate liquid is cooled, its viscosity will progressively increase. In the vicinity of the glass transition temperature, T_g, the viscosity shows a marked temperature dependence. T_g is commonly determined from the sharp change in heat capacity occurring at the transition, as a result of a change from liquidlike to solidlike behavior over the experimental time scale. For a low molecular weight material, a typical value of the shear viscosity at T_g is $\sim 10^{12}$ Pa s, giving an associated structural relaxation time of ~100 s. For a polymeric material, the large change in structural relaxation time results in a change from rubbery to brittle behavior, as the material is cooled through T_g. As cooling is continued below T_g, the structural relaxation time will continue to increase.

The density of most amorphous materials increases with decreasing temperature. Vitrification at T_g effectively "locks in" a liquid structure, and the expected densification on cooling subsequently occurs at a rate related to the structural relaxation time. As a consequence of the slow densification, material properties, including compliance, stiffness, and brittleness (*13*), slowly evolve with time, with the whole process commonly known as physical aging. The densification can also slow diffusion of low molecular weight species within the glass (*14*), although conversely the embrittlement and potential fracture of the glassy matrix may also make it more permeable.

The structural relaxation time is in part dependent on temperature and partly on liquid structure. Liquid structure is characterized on a temperature scale through the notion of a fictive temperature, T_f, the temperature at which a particular structure would be fully relaxed (*15*). Densification affects the energetics of interaction between molecules and the accessibility of liquid configurations, both of which can be probed in a calorimetric experiment. The calorimetric consequence of the slow structural relaxation, which occurs on aging in the glass, is observed as a peak in heat capacity preceding T_g or an overshoot at T_g on subsequent heating.

There are various phenomenological approaches for describing the observed time-dependent behavior; a widely applied one, which has a potentially useful predictive capability, is the Tool−Narayanaswamy−Moynihan (TNM) (*9*, *10*, *15*, *16*) method, which has been applied to polymeric systems. The dependence of structural relaxation on time, t, can be described by an empirical relaxation function, ϕ, of the stretched exponential form

* To whom correspondence should be addressed. Tel: +44(0)1603 255000. Fax: +44(0)1603 507723. E-mail: steve.ring@bbsrc.ac.uk.
† Institute of Food Research.
‡ University of Nottingham.

10.1021/jf0580770 CCC: $30.25
Published on Web 10/04/2005

$$\phi(t) = \exp[-(t/\tau_0)^{\beta}] \quad (1)$$

and β ($0 < \beta \leq 1$) is a measure of its nonexponentiality. τ_0 is a characteristic time, which is dependent on both temperature, T, and, to an extent, liquid structure (characterized by T_f), and has been successfully obtained using the expression

$$\tau_0 = A \exp[x\Delta h^*/RT + (1-x)\Delta h^*/RT_f] \quad (2)$$

where A, x ($0 < x \leq 1$), and Δh^* are constants (*16*−*18*). These relationships can be used to calculate the time dependence of T_f following a temperature step. The cooling and heating of a sample can be considered as a succession of n such steps in which case

$$T_{f,n} = T_0 + \sum_{j=1}^{n} \Delta T_j \{1 - \exp[-(\sum_{k=j}^{n} \Delta T_k/Q\tau_{0,k})^{\beta}]\} \quad (3)$$

where Q is a heating or cooling rate and T_0 is a starting temperature where relaxation is sufficiently rapid that, in the initial stages of cooling, equilibrium is obtained. During annealing, the sample is held at a fixed temperature, T_a; for a certain length of time, this is divided into 10 logarithmically spaced steps with eq 3 being modified as described

$$T_{f,n} = T_0 + \sum_{j=1}^{n_a} \Delta T_j \{1 - \exp[-(\sum_{k=n_a}^{n} \Delta t_{e,k}/\tau_{0,k})^{\beta}]\} \quad (4)$$

where $n_a + 10 \geq n > n_a$ and

$$\Delta t_{e,k} = t_e^{1/10} \quad k = n_a + 1$$

$$\Delta t_{e,k} = t_e^{(k-n_a)/10} - t_e^{(k-n_a-1)/10} \quad k > n_a + 1$$

For a calorimetric experiment, $T_{f,n}$ is then related to a normalized heat capacity, $C_{p,n}$, by

$$C_{p,n} = (T_{f,n} - T_{f,n-1})/(T_n - T_{n-1}) \quad (5)$$

These predicted values of $C_{p,n}$ can then be compared with those determined calorimetrically.

A potential advantage of the above approach is that once the various parameters describing the observed calorimetric behavior are obtained, it can be used to predict the effects of changing storage time and temperature. In an earlier study, we found the TNM method useful in modeling the calorimetric behavior of dry amorphous maltose (*4*), and it has also been applied by other workers in the study of amorphous glucose and fructose (*5*). This approach is potentially of greater practical utility if the changes in calorimetric behavior are related to the observed changes in mechanical behavior. This study aims to characterize and compare the structural relaxation behavior of low water content maltose, maltodextrin, and starch materials, using calorimetry and mechanical testing. The study then examines the usefulness of the TNM approach for describing the observed time-dependent calorimetric behavior and its relationship to mechanical properties.

MATERIALS AND METHODS

Materials. All chemicals used were of analytical grade. Crystalline maltose monohydrate was obtained from Sigma and had a water content of 5% w/w on a wet weight basis. Maltodextrin (DE 29) was obtained as a gift from Roquette. Starch-rich extrudates were obtained as a gift from PepsiCo. The extrudates contained more than 90% w/w potato starch and were prepared by (i) mixing the raw materials into a dough, (ii) extruding the dough into a sheet using a pasta extruder, (iii) steaming the dough to gelatinize the starch, and (iv) drying to a half product.

Fabrication of Bars. Maltose/water mixtures were prepared by melting a mixture of maltose monohydrate (50 g) and water (30 g) in a weighed stainless steel beaker on a hotplate, using an infrared lamp to heat the surface layer. The water content of the sample was reduced by boiling. The beaker and sample were weighed at regular intervals until the desired water content was obtained. Bars were fabricated in a mold (50 mm long × 10 mm wide) lined with cellulose acetate (0.5 mm thick). A 1.5 mL amount of molten maltose/water mixture was drawn up into a preheated syringe (80 °C) and extruded into the preheated mold, taking care not to introduce air bubbles. The mold was allowed to cool to room temperature, and the bar was removed and stored in dry silicone oil (Dow Corning 710, Merck). The variation in water content during batch preparation was monitored by differential scanning calorimetry (DSC), through the determination of the glass transition temperature, T_g (*11*). Using this method, the upper maltose content limit was 96% w/w due to problems of molding and obtaining bubble-free samples from more viscous, higher solids content melts. Maltodextrin/water bars were prepared in the same way as the maltose/water bars. Extruded starch bars (40 mm × 12 mm × 1 mm) conditioned to 89% w/w solids over a salt solution were heated to 20 °C above T_g and then pressed between Teflon-coated metal blocks to give flat samples suitable for a three-point bend test.

Mechanical Measurements. The mechanical behavior of rectangular bars was examined in a three-point bend test over a span of 25 mm using an Instron 1122 material tester with a 250 N load cell. Prior to testing, a bar was heated in dry silicone oil at a temperature 15 °C above its T_g for 10 min to remove the effects of prior thermal history. After heating, the bath was cooled on ice and the temperature was monitored until it reached the T_g of the bar (~10 min). The bar was then positioned on the test fixture, immersed in a purpose-built silicone oil bath, and held at the aging temperature, T_a. To allow for thermal equilibration, the first measurement was performed at an aging time, t_a, of 20 min. The crosshead of the material tester was lowered at a rate of 2 mm min^{-1}, and the load cell response was logged by computer at a rate of 50 Hz until the desired force was reached. For relaxation studies, the applied strain was kept within the linear limit and was typically 0.1%. The crosshead was stopped, and the load cell response was logged for every 0.25% change in signal. The time of deformation was approximately 2 s, and the duration of each mechanical test was less than 10% of the total aging time t_a. Measurements were performed at aging times of 20, 40, 80, 160, and 320 min. Between measurements, the sample was not moved from the fixture. The stress, σ (in Pa), and strain, ϵ (dimensionless), were calculated using the following relationships

$$\sigma = 3Fl/2bh^2 \quad (6)$$

$$\epsilon = 6hY/l^2 \quad (7)$$

where F is the load (in N); l, b, and h are the load support span, sample breadth, and height (all in m), respectively; and Y is the deflection at the load nose (in m). The flexural modulus, E_F (in Pa), is given by

$$E_F = \sigma/\epsilon \quad (8)$$

and was calculated from the slope of stress vs strain.

Differential Scanning Calorimetry (DSC). The T_g of samples was determined by calorimetry using a Perkin-Elmer DSC7 fitted with a robotic autosampler and an Intra-cooler II. The instrument was calibrated for temperature using the melting temperatures of indium (156.6 °C), dodecane (−9.65 °C), and octadecane (28.24 °C) and for heat flow using the heat of fusion of indium (28.45 J g^{-1}). The instrument was calibrated for heat capacity, C_p, using a sapphire standard. Material (5−10 mg) was cut from the center of the rectangular bars and quickly sealed in aluminum sample pans (50 μL) and weighed. Values of T_g were determined for all samples using data obtained on the second scan following heating to remove prior thermal history where T_g was defined as the midpoint of the heat capacity increment at the

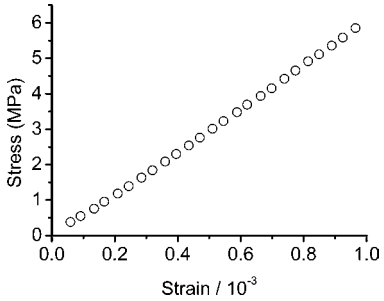

Figure 1. Stress strain plot for a 96% w/w maltose/water mixture at 30 °C ($T_g - T$ of 12 °C).

glass transition using Perkin-Elmer software. Samples were scanned over the range $T_g \pm 30$ °C at a rate of 10 °C/min. The T_g values of the samples were as follows: 94% w/w maltose/water, 24 °C; 95% w/w maltose/water, 31 °C; 96% w/w maltose/water, 42 °C; 89% w/w maltodextrin/water, 20 °C; and 89% w/w starch/water, 50 °C.

Calorimetric aging studies were performed by heating the sample to 30 °C above T_g to abolish the effects of prior thermal history, quenching to the aging temperature T_a, where it was held for a time, t_a (0−320 min), and then quenched to 30 °C below T_g and then scanned to 30 °C above T_g. Δh^* was determined by the dependence of T_f on cooling rate using Perkin-Elmer software. A sample was cooled from $T_g + 30$ °C to $T_g - 30$ °C at rates ranging from 0.1 to 30 °C/min followed by reheating at 10 °C/min. The enthalpy change on aging, ΔH, was determined by integration of the overshoot in heat capacity in the vicinity of T_g, through comparison of aged and minimally aged samples, i.e., the aging during cooling and immediate reheating of the sample in the calorimeter.

RESULTS AND DISCUSSION

Mechanical Behavior. The glass transition behavior of carbohydrates shows a strong dependence on water content (*12*, *19*), and there is a need for rigorous control of water content in mechanical testing. This includes minimizing the uptake of moisture during sample transfer, which can result in surface plasticization, and was revealed as nonlinearity in stress/strain plots at small deformations. In the present study, water uptake was controlled by storing the samples in dry silicone oil and carrying out the mechanical testing under silicone oil. **Figure 1** shows a stress/strain plot for a 96% w/w maltose/water bar aged for 20 min at 30 °C. The flexural modulus, E_F, determined from the slope of the stress/strain plot, was 6.0×10^9 N m^{-2}. The observed modulus was characteristic of glassy materials.

At the deformation rate used in the three-point bend test, the determination of E_F was complete within 1 s. To probe the structural rearrangement within the glass on deformation and the effect of aging on this behavior, the relaxation modulus, E_{Frelax}, was determined as a function of time, from 0 to ∼1000 s, and as a function of aging time, t_a. The time dependence of E_{Frelax}, was determined for strains of ∼0.001, within the linear region of the stress/strain plot (**Figure 1**). The dependence of E_{Frelax} on time and t_a for maltose/water, maltodextrin/water, and starch/water mixtures is shown in **Figure 2a**−**c**, respectively.

The materials behaved in the same general way. Initial values of E_F were characteristic of glassy solids and increased in the order starch < maltodextrin < maltose. The mechanical relaxation could be fitted to a relaxation function of the same stretched exponential form as the structural relaxation (eq 1), i.e.,

$$\phi(t) = \exp[-(t/\tau_{0,m})^{\beta}] \quad (9)$$

where β ($0 < \beta < 1$) is a measure of its nonexponentiality and $\tau_{0,m}$ is a characteristic mechanical relaxation time. For all data

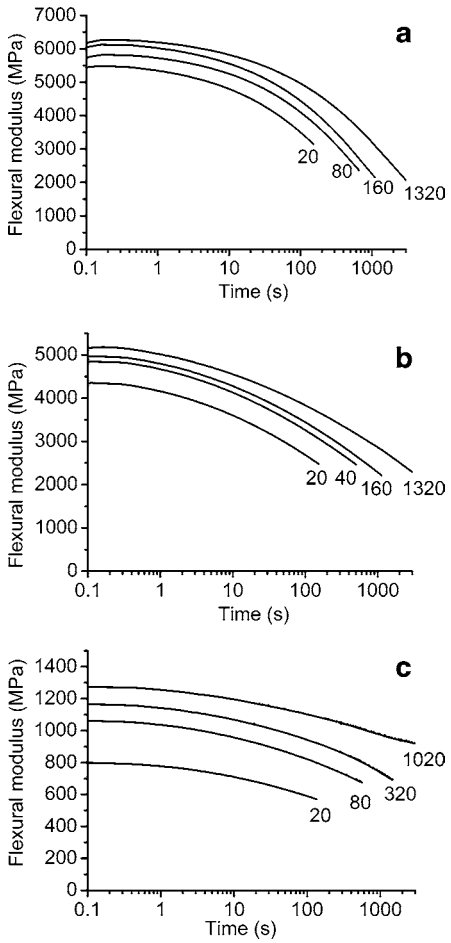

Figure 2. (**a**) Stress relaxation of a 96% w/w maltose/water mixture aged at 30 °C ($T_g - T$ of 12 °C) for 20–1320 min. (**b**) Stress relaxation of an 89% w/w maltodextrin/water mixture aged at 8 °C ($T_g - T$ of 12 °C) for 20–1320 min. (**c**) Stress relaxation of an 89% w/w starch/water mixture aged at 32 °C ($T_g - T$ of 18 °C) for 20–1020 min.

sets of mechanical behavior, the fittings gave a $r^2 > 0.997$. With increasing aging time, t_a, the initial value of E_{Frelax} and $\tau_{0,m}$ increased. The values of the parameter β range from 0.49 to 0.55 for the maltose/water mixture, 0.38 to 0.42 for the maltodextrin/water mixture, and 0.34 to 0.40 for the starch/water mixture (**Table 1**). The dependence of $\tau_{0,m}$ on the degree of quench below T_g for a maltose/water mixture is shown in **Figure 3a** as a double logarithmic plot. $\tau_{0,m}$ increases with an increase in t_a and with an increase in depth of quench (expressed as $T_g - T$) below T_g. Over the range of aging times examined, log $\tau_{0,m}$ shows an approximately linear dependence on log t_a ($r^2 > 0.95$). The dependence of $\tau_{0,m}$ on t_a for a maltose/water, maltodextrin/water, and starch/water mixture is shown in **Figure 3b**. The main determinant of $\tau_{0,m}$ and its evolution on aging is the depth of quench below T_g. Starch/water and maltodextrin/water mixtures showed similar behavior to maltose/water mixtures at the same degree of quench. The changes in mechanical relaxation behavior with t_a are characteristic of the phenomenon of physical aging through slow structural relaxation (*10*, *13*).

Calorimetric Measurements. A comparison of the calorimetric behavior of minimally aged and aged samples of maltose/water, maltodextrin/water, and starch/water mixtures is shown in **Figure 4a**−**c**, respectively, where normalized heat capacity, $C_{p,n}$, is plotted as a function of temperature. For all samples, an increment in $C_{p,n}$ is observed at the calorimetric transition

Table 1. Fitting Parameters for Mechanical and Calorimetric Relaxation Behavior of Aged Maltose/Water, Maltodextrin/Water, and Starch/Water Mixtures[a]

sample (solid content)	aging conditions		mechanical relaxation[b]		calorimetric relaxation[c]		
	T (°C)	t_a (min)	$\tau_{0,m}$ (s)	β	x	β	ln A
maltose/water	30	40	607	0.52	0.475	0.46	−180.0
(96% w/w)	30	80	791	0.51	0.475	0.43	−180.0
	30	160	990	0.50	0.475	0.40	−180.0
	30	320	1290	0.49	0.475	0.37	−180.0
maltodextrin/water	8	40	621	0.42	0.315	0.27	−191.5
(89% w/w)	8	160	1556	0.38	0.315	0.26	−191.5
starch/water	32	40	2534	0.40	0.37	0.25	−173.5
(89% w/w)	32	160	7755	0.34	0.37	0.24	−173.5

[a] The calorimetric parameter, Δh^*, was fixed at 480 kJ mol^{-1}. [b] Parameters determined by fitting normalized relaxation modulus to eq 9. [c] Calorimetric β parameter determined by fitting normalized heat capacity to TNM model (eqs 1–5).

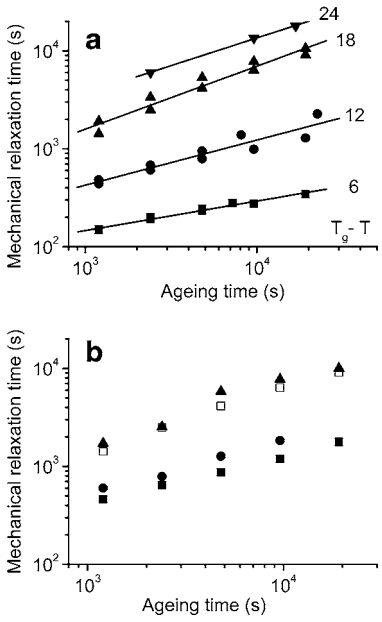

Figure 3. (**a**) Effect of aging and degree of quench below T_g on mechanical relaxation time for a 96% w/w maltose/water mixture. (**b**) Dependence of mechanical relaxation time on aging time for a starch/water ($T_g - T$ of 18 °C) (▲); maltodextrin/water ($T_g - T$ of 12 °C) (●); and maltose/water mixture with a $T_g - T$ of 12 (■) and 18 (□) °C.

temperature T_g. While the heat capacity increment is relatively sharp for the maltodextrin and maltose/water mixtures, the observed transition for the starch sample is broader. On aging, an overshoot in heat capacity is observed for all of the materials tested. This overshoot is characteristic of physical aging through structural relaxation and is commonly referred to as enthalpy relaxation (*5*, *15*, *17*, *20*). From comparison of the heat capacities of aged and minimally aged samples, it was possible to determine, by integration, an enthalpy change, ΔH, for this overshoot. For the materials examined, ΔH increased in the order starch < maltodextrin < maltose and showed a linear increase with the logarithm of the aging time, t_a (**Figure 5**).

It is useful to consider the relationship between the changes in mechanical and calorimetric behavior. In many polymeric systems, no simple correlation is observed and is attributed to the different physical origins of the two behaviors (*10*, *20*). In the present study, there was a relationship between the magnitude of the structural relaxation probed by mechanical

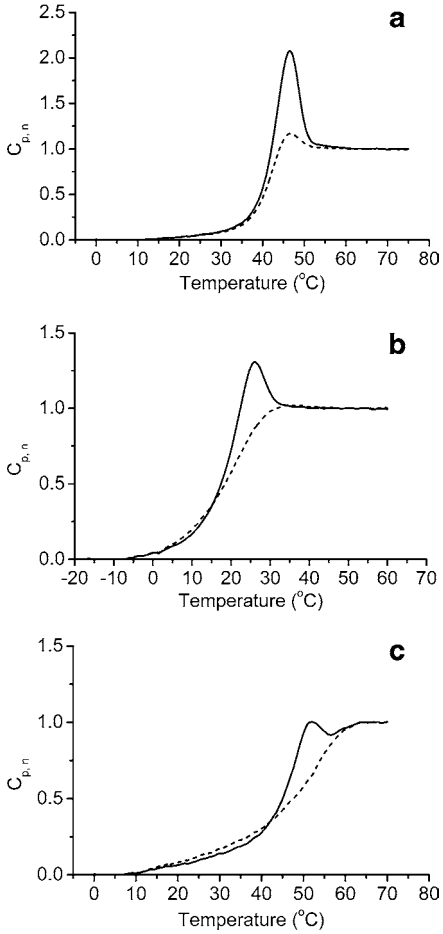

Figure 4. (**a**) Plot of normalized heat capacity, $C_{p,n}$, of a 96% w/w maltose/water mixture as a function of temperature for a sample stored at 30 °C ($T_g - T$ of 12 °C) for 0 (- - -) and 160 (—) min. (**b**) Plot of normalized heat capacity, $C_{p,n}$, of an 89% w/w maltodextrin/water mixture as a function of temperature for a sample stored at 8 °C ($T_g - T$ of 12 °C) for 0 (- - -) and 160 (—) min. (**c**) Plot of normalized heat capacity, $C_{p,n}$, of an 89% w/w starch/water mixture aged at 32 °C for 0 (- - -) and 160 (—) min.

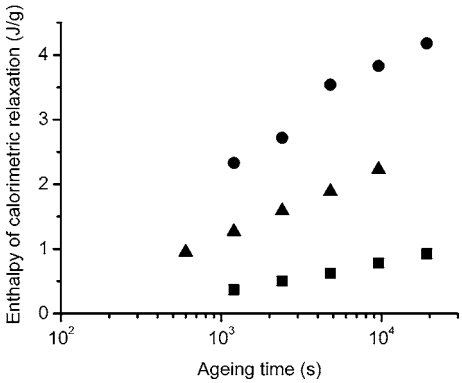

Figure 5. Dependence of enthalpy of calorimetric relaxation on aging time for maltose/water (●), maltodextrin/water (■), and starch/water mixtures (▲).

measurement and the observed extent of aging as probed by calorimetry. The slower the development of the calorimetric effect, the slower the mechanical relaxation. One of the potentially most straightforward correlations to attempt is to relate ΔH to a change in mechanical behavior. For the materials examined, a correlation was found between log τ_0 and ΔH (**Figure 6**) with values of r^2 for maltose/water 0.94, maltodextrin/water 0.99, and starch/water 0.96.

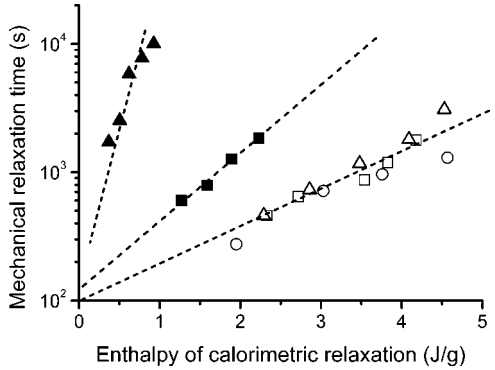

Figure 6. Correlation of mechanical relaxation time with enthalpy of calorimetric relaxation for 96% w/w maltose/water ($T_g - T$ of 12 °C) (□), 95% w/w maltose/water ($T_g - T$ of 12 °C) (△), 94% w/w maltose/water ($T_g - T$ of 12 °C) (○), 89% w/w maltodextrin/water ($T_g - T$ of 12 °C) (■), and 89% w/w starch/water mixtures ($T_g - T$ of 18 °C) (▲).

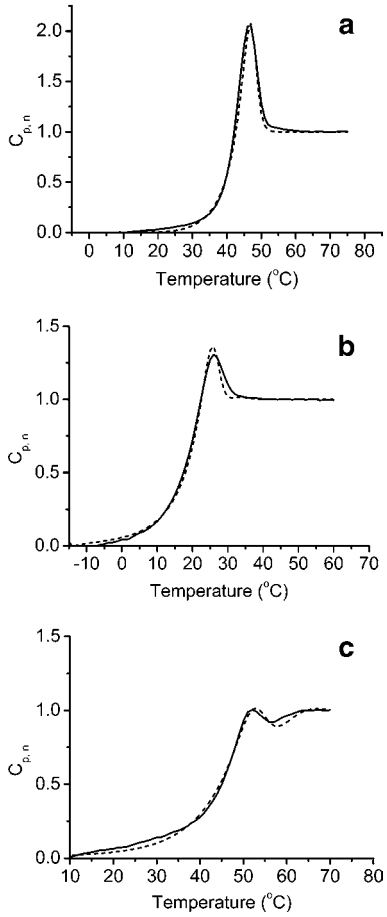

Figure 7. (**a**) Comparison of experimental and calculated normalized heat capacity, as a function of temperature for a 96% w/w maltose/water mixture stored at 30 °C ($T_g - T$ of 12 °C) for 160 min. (**b**) Comparison of experimental and calculated normalized heat capacity, as a function of temperature for an 89% w/w maltodextrin/water mixture stored at 8 °C ($T_g - T$ of 12 °C) for 160 min. (**c**) Comparison of experimental and calculated normalized heat capacity, as a function of temperature for an 89% w/w starch/water mixture stored at 32 °C ($T_g - T$ of 18 °C) for 160 min.

A more detailed examination of the calorimetric behavior was also attempted using the TNM model. Examples of the usefulness of this approach for describing the calorimetric data are shown in **Figure 7a−c** for maltose/water, maltodextrin/water, and starch/water mixtures, respectively. For all of the materials, the TNM approach gives a good description of the observed behavior. The values of the various parameters used to describe the behavior are summarized in **Table 1**. The parameters of the TNM approach are strongly correlated, which can make the optimization of the fitting difficult (*15*). When Δh^* is fixed, the value of ln A is tightly constrained. Δh^* was obtained independently from the dependence of the calorimetric T_f on scanning rate, and then, ln A was obtained by fitting unaged data. The nonlinearity parameter, x, was estimated using the method of Hutchinson et al. (*20*), and the parameter, β, varied to obtain fittings shown. Although there is an association between mechanical and calorimetric relaxation, the parameter, β, describing the nonexponentiality of the relaxation is different for the two processes.

In conclusion, the physical aging of glassy, low moisture content, starch/water, maltodextrin/water, and maltose/water mixtures is broadly comparable. Physical aging results in an increase in stiffness of the materials and a shift in the mechanical relaxation to longer times. In calorimetric experiments, the extent of physical aging is revealed as an overshoot in heat capacity in the vicinity of the calorimetric glass transition. For the materials examined, the time-dependent change in ΔH of the overshoot can be correlated to the change in mechanical relaxation time. The observed calorimetric behavior is well-described by the TNM method, which may be used to give predictions on the time and temperature dependence of physical aging. We have demonstrated a coherent approach, which can be applied to understand and predict physical aging in the mechanical properties of glassy food materials. This is relevant to applications such as textural change of glassy food products and the mechanical stability of glassy encapsulation matrices.

LITERATURE CITED

(1) Miles, M. J.; Morris, V. J.; Orford, P. D.; Ring, S. G. The roles of amylose and amylopectin in the gelation and retrogradation of starch. *Carbohydr. Res.* **1985**, *135*, 271−281.

(2) Shogren, R. L. Effect of moisture-content on the melting and subsequent physical aging of corn starch. *Carbohydr. Polym.* **1992**, *19*, 83−90.

(3) Lammert, A. M.; Lammert, R. M.; Schmidt, S. J. Physical aging of maltose glasses as measured by standard and modulated differential scanning calorimetry. *J. Therm. Anal. Calorim.* **1999**, *55*, 949−975.

(4) Noel, T. R.; Parker, R.; Ring, S. M.; Ring, S. G. A calorimetric study of structural relaxation in a maltose glass. *Carbohydr. Res.* **1999**, *319*, 166−171.

(5) Wungtanagorn, R.; Schmidt, S. J. Phenomenological study of enthalpy relaxation of amorphous glucose, fructose and their mixture. *Thermochim. Acta* **2001**, *369*, 95−116.

(6) Lourdin, D.; Colonna, P.; Brownsey, G. J.; Noel, T. R.; Ring, S. G. Structural relaxation and physical aging of starchy materials. *Carbohydr. Res.* **2002**, *337*, 827−833.

(7) Borde, B.; Bizot, H.; Vigier, G.; Buleon, A. Calorimetric analysis of the structural relaxation in partially hydrated amorphous polysaccharides. II. Phenomenological study of physical aging. *Carbohydr. Polym.* **2002**, *48*, 111−123.

(8) Chung, H. J.; Lim, S. T. Physical aging of glassy normal and waxy rice starches: Effect of aging time on glass transition and enthalpy relaxation. *Food Hydrocolloids* **2003**, *17*, 855−861.

(9) Hodge, I. M. Physical aging in polymer glasses. *Science* **1995**, *267*, 1945−1947.

(10) Hutchinson, J. M. Physical aging of polymers. *Prog. Polym. Sci.* **1995**, *20*, 703−760.

(11) Orford, P. D.; Parker, R.; Ring, S. G.; Smith, A. C. Effect of water as a diluent on the glass transition behaviour of malto-oligosaccharides, amylose and amylopectin. *Int. J. Biol. Macromol.* **1989**, *11*, 91−96.

(12) Zeleznak, K. J.; Hoseney, R. C. The glass transition in starch. *Cereal Chem.* **1987**, *64*, 121−124.
(13) Struik, L. C. E. *Physical Aging in Amorphous Polymers and Other Materials*; Elsevier: Amsterdam, 1978.
(14) Zhang, J.; Wang, C. H. Application of the laser-induced holographic grating relaxation technique to the study of physical aging of an amorphous polymer. *Macromolecules* **1987**, *20*, 683−685.
(15) Hodge, I. M. Enthalpy relaxation and recovery in amorphous materials. *J. Non-Cryst. Solids* **1994**, *169*, 211−266.
(16) Moynihan, C. T.; Crichton, S. N.; Opalka, S. M. Linear and nonlinear structural relaxation. *J. Non-Cryst. Solids* **1991**, *131*, 420−434.
(17) Berens, A. R.; Hodge, I. M. Effects of annealing and prior history on enthalpy relaxation in glassy polymers.1. Experimental study on poly(vinyl chloride). *Macromolecules* **1982**, *15*, 756−761.
(18) Hodge, I. M.; Berens, A. R. Calculation of the effects of annealing on sub T_g endotherms. *Macromolecules* **1981**, *14*, 1598−1599.
(19) Orford, P. D.; Parker, R.; Ring, S. G. Aspects of the glass transition behaviour of carbohydrates of low molecular weight. *Carbohydr. Res.* **1990**, *196*, 11−18.
(20) Hutchinson, J. M.; Smith, S.; Horne, B.; Gourlay, G. M. Physical aging of polycarbonate: Enthalpy relaxation, creep response, and yielding behavior. *Macromolecules* **1999**, *32*, 5046−5061.

Received for review March 30, 2005. Revised manuscript received August 11, 2005. Accepted August 18, 2005. We thank DEFRA for financial support. S.G.R., T.R.N., G.J.B. and R.P. thank the BBSRC core strategic grant for financial support.

JF0580770